

Photoinduced Dissociative Electron Transfer: Is the Quantum Yield Theoretically Predicted to Equal Unity?

Marc Robert and Jean-Michel Savéant*

Contribution from the Laboratoire d'Electrochimie Moléculaire, Unité Mixte de Recherche Université - CNRS No. 7591, Université de Paris 7 - Denis Diderot, 2 place Jussieu, 75251 Paris Cedex 05, France

Received August 2, 1999. Revised Manuscript Received October 26, 1999

Abstract: An attractive manner of fighting back-electron transfer to the ground state in photoinduced electron transfer reactions is to use a system in which the donor and/or the acceptor in the ion-pair undergoes a rapid fragmentation. Intuitively, it seems that an ideal situation in this respect, leading to a unity quantum yield, should be met when fragmentation and electron transfer are concerted. Accordingly, a quantum yield below 1 would be the signature of a nonconcerted two-step mechanism. It is shown, from first principles, that a purely dissociative photoinduced electron transfer is not necessarily endowed with a unity quantum yield. The reason is that the system partitions between fragmentation and back-electron transfer in the funnel offered by the upper first-order potential energy surface combining the ground state and fragments zero-order surfaces. A semiclassical model is presented, relating the quantum yield to the electronic matrix coupling element, H . Only in the case of a completely nonadiabatic ground-state electron transfer ($H = 0$) should the quantum yield reach unity. Upon increasing H , the quantum yield rapidly decreases to a distinctly smaller value which can be as low as 0.5.

An attractive way of fighting energy-wasting back-electron transfer in photoinduced electron-transfer reactions is to use a system where either the acceptor or the donor in the resulting ion-pair, or both, undergo a fast cleavage reaction.¹ The occurrence of a concerted electron-transfer/bond-breaking reaction (henceforth called dissociative electron transfer) rather than a stepwise reaction (as illustrated in Scheme 1 for a reductive cleavage reaction) thus intuitively appears as an extreme and ideal situation where the complete quenching fragmentation quantum yield, Φ_{∞} , should be unity.^{1,2} From a diagnosis standpoint, the observation of a quantum yield smaller than unity would thus rule out the occurrence of a dissociative electron-transfer mechanism.² So far no example of unity quantum yields involving an acceptor or a donor containing a frangible bond has been reported. On the basis of the aforementioned intuition, the intermediacy of a discrete ion radical was thus inferred in these systems.^{1c,2,3} In contrast, the occurrence of thermal, electrochemical, or homogeneous dissociative electron transfers is well documented.^{4–6} The transition between the concerted and stepwise mechanisms upon changing the molecular structure within the same family of compounds has been observed in a number of cases.^{5,6} Several examples have also been reported

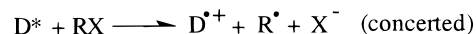
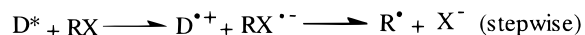
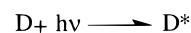
(1) (a) Saeva, F. D. *Top. Curr. Chem.* **1990**, *156*, 61. (b) Saeva, F. D. Intramolecular Photochemical Electron Transfer (PET)-Induced Bond Cleavage Reactions in some Sulfonium Salts Derivatives. In *Advances in Electron-Transfer Chemistry*; Mariano, P. S., Ed.; JAI Press: New York, 1994; Vol. 4, pp 1–25. (c) Gaillard, E. R.; Whitten, D. G. *Acc. Chem. Res.* **1996**, *29*, 292.

(2) (a) Arnold, B. R.; Scaiano, J. C.; McGimpsey, W. G. *J. Am. Chem. Soc.* **1992**, *114*, 9978. (b) Chen, L.; Farahat, M. S.; Gaillard, E. R.; Gan, H.; Farid, S.; Whitten, D. G. *J. Am. Chem. Soc.* **1995**, *117*, 6398. (c) Wang, X.; Saeva, F. D.; Kampmeier, J. A. *J. Am. Chem. Soc.* **1999**, *121*, 4364.

(3) Chen, L.; Farahat, M. S.; Gaillard, E. R.; Farid, S.; Whitten, D. G. *J. Photochem. Photobiol., A* **1996**, *95*, 21.

(4) (a) Savéant, J.-M. Single Electron Transfer and Nucleophilic Substitution. In *Advances in Physical Organic Chemistry*; Bethel, D., Ed.; Academic Press: New York, 1990; Vol. 26, pp 1–130. (b) Savéant, J.-M. Dissociative Electron Transfer. In *Advances in Electron-Transfer Chemistry*; Mariano, P. S., Ed.; JAI Press: New York, 1994; Vol. 4, pp 53–116.

Scheme 1



The same formalism applies to the reduction of a +n charged substrate (with X^{n+} replacing X) and to the oxidation of a -n charged substrate (with X^{n-} replacing X)

where the two mechanisms have been observed with the same cleaving acceptor molecule, thus demonstrating without ambiguity the reality of the concerted pathway. It has indeed been found that the passage from the concerted to the stepwise mechanism may be triggered by an increase of the driving force of the reaction, as expected on theoretical grounds.⁷ The increase in driving force was achieved by changing the electrode potential and the standard potential of the donor in electrochemical^{5c,6c,8} and homogeneous examples^{5f,9} respectively.

(5) (a) Andrieux, C. P.; Le Gorande, A.; Savéant, J.-M. *J. Am. Chem. Soc.* **1992**, *114*, 6892. (b) Andrieux, C. P.; Differding, E.; Robert, M.; Savéant, J.-M. *J. Am. Chem. Soc.* **1993**, *115*, 6592. (c) Andrieux, C. P.; Robert, M.; Saeva, F. D.; Savéant, J.-M. *J. Am. Chem. Soc.* **1994**, *116*, 7864. (d) Andrieux, C. P.; Tallec, A.; Tardivel, R.; Savéant, J.-M.; Tardy, C. *J. Am. Chem. Soc.* **1997**, *119*, 2420. (e) Andrieux, C. P.; Savéant, J.-M.; Tardy, C.; Savéant, J.-M. *J. Am. Chem. Soc.* **1997**, *119*, 11546. (f) Costentin, C.; Hapiot, P.; Médebielle, M.; Savéant, J.-M. *J. Am. Chem. Soc.* **1999**, *121*, 4451.

(6) (a) Workentin, M. S.; Maran, F.; Wayner, D. D. M. *J. Am. Chem. Soc.* **1995**, *117*, 2120. (b) Antonello, S.; Musumeci, M.; Wayner, D. D. M.; Maran, F. *J. Am. Chem. Soc.* **1997**, *119*, 9541. (c) Antonello, S.; Maran, F. *J. Am. Chem. Soc.* **1997**, *119*, 12595. (d) Workentin, M. S.; Donkers, R. L. *J. Am. Chem. Soc.* **1998**, *120*, 2664.

(7) (a) Andrieux, C. P.; Savéant, J.-M. *J. Electroanal. Chem.* **1986**, *205*, 43. (b) The displacement of the potential energy surfaces resulting in the change of mechanism is sketched, for example, in Figure 5 of ref 7a or Figure 1 of ref 5a.

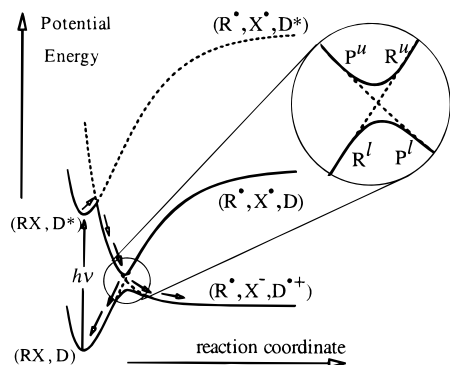


Figure 1. Section of the zero-order (···) and first-order (—) potential energy surfaces along the reaction coordinate in cases where stretching of the cleaving bond is the dominant factor of nuclei reorganization.

There are a few, but remarkable, examples where, for the same cleaving acceptor, the photochemical reaction was deemed, based on a quantum yield smaller than unity, to follow a stepwise mechanism, whereas the electrochemical reaction was reported to follow a concerted mechanism. One concerns the reaction of benzyl and 4-cyanobenzyl bromides with the excited state of the diphenylmethyl radical^{2a} or of pinacols^{2b} and the other, the reductive cleavage of the 4-cyanobenzylmethylphenyl sulfonium cation by the excited singlets of a series of aromatic compounds.^{2c} For all of these compounds, the electrochemical reductive cleavage appears to follow a concerted mechanism.^{5a,c} The later example is particularly interesting because great care was taken, by appropriate choice of the donors, to avoid the occurrence of electron transfer between the donor cation radical and the 4-cyanobenzyl radical, followed by regeneration of the starting sulfonium cation by coupling of the resulting 4-cyanobenzyl cation with methylphenyl sulfide, thus wasting the photochemical energy. Avoiding this type of side-reaction is crucial in studies aiming at relating the quantum yield and the dissociative character of the electron-transfer/bond-breaking process.

How can these photochemical and electrochemical data be reconciled? With the benzylic molecules under discussion, electron transfer may involve the π^* or the σ^* orbital, giving rise to a stepwise and concerted mechanism, respectively. This is a typical case where the mechanism is a function of the driving force of the reaction as evoked earlier. Since the photochemical reactions are strongly downhill, whereas the electrochemical reaction is slightly uphill, the mechanism may change from stepwise in the first case to concerted in the second. However, regardless of the validity of this interpretation, we wish to address here a more fundamental question, namely: *is it true, from first principles, that a purely dissociative photoinduced electron transfer is necessarily endowed with a unity quantum yield?*

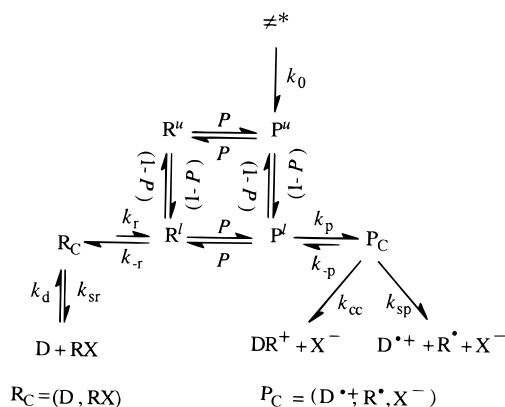
Results and Discussion

Figure 1 shows the potential energy diagram of the three states involved for simplified systems in which the stretching of the cleaving bond is the dominant factor of the nuclei reorganization taking place upon electron transfer. In many cases this condition is approximately achieved. Typical relative contributions to the

(8) (a) Another striking example of transition between concerted to stepwise mechanisms has been found very recently in the electrochemical reduction of iodobenzene.^{8b} (b) Pause, L.; Robert, M.; Savéant, J.-M. *J. Am. Chem. Soc.* **1999**, *121*, 7158.

(9) Severin, M. G.; Farnia, E.; Vianello, E.; Arévalo, M. C. *J. Electroanal. Chem.* **1988**, *251*, 369.

Scheme 2



intrinsic barrier are indeed 80% for bond cleavage and 20% for solvent reorganization.⁴ After overcoming a small activation barrier, the system approaches the region where the ground state and fragments zero-order surfaces cross each other, that is, the region where the transition state of the thermal electron transfer between the donor ground state and the cleaving acceptor is located. The system would proceed exclusively to the fragmented products only if the electronic matrix coupling element at the intersection, H , is nil, that is, if the ground-state electron transfer is purely nonadiabatic. If this is not the case, the system will partition between back-electron transfer and fragmentation through the funnel offered by the upper first-order surface leading to a value of the quantum yield smaller than unity.

A semiclassical treatment¹⁰ of the model depicted in Figure 1, based on the Morse curve theory of thermal dissociative electron transfer,^{4,11} allows the prediction of the quantum yield as a function of the electronic matrix coupling element, H . The various states to be considered in the region where the zero-order potential energy curves cross each other are shown in the insert of Figure 1. Their fate is depicted by the kinetic Scheme 2.¹² P^u , on the upper first-order curve is formed from the transition state of the photoinduced reaction, \neq^* , at a rate, k_0 , $= I/V$ (I : light intensity, V : volume of the solution). The probability, P , that the system remains on the upper first-order curve, thus yielding R^u reversibly, is a rapidly increasing function of the electronic coupling matrix element, H (see eq 3 below). The probability that the system crosses the intersection while remaining on the zero-order curve, thus yielding P^l reversibly, is $(1 - P)$. Likewise, the reversible interconversion of R^u and R^l occurs with a probability $(1 - P)$ in both directions. These probabilities may be converted into rate constants by multiplication by ν_{eff} , the effective frequency at which the system crosses the intersection region (for an expression of ν_{eff} , see Supporting Information). On the reactant curve, R^l relaxes to the ground-state caged reactant system, R_C , with a rate constant k_{-r} , while R^l may be regenerated from R_C with a rate constant k_r .

$$k_r/k_{-r} = \exp(-F\Delta G_{\text{r}}^{\ddagger}/RT) = k_{\text{act}}/\nu_{\text{eff}}$$

($\Delta G_{\text{r}}^{\ddagger}$ is the activation free energy for the ground-state dis-

(10) (a) Landau, L. *Phys. Z. Sowjetunion* **1932**, *2*, 46. (b) Zener, C. *Proc. R. Soc. London, Ser. A* **1932**, *137*, 696. (c) Hush, N. S. *Electrochim. Acta* **1968**, *13*, 1005. (d) Newton, M. D.; Sutin, N. *Annu. Rev. Phys. Chem.* **1984**, *35*, 437. (e) Brunschwig, B. S.; Logan, J.; Newton, M. D.; Sutin, N. *J. Am. Chem. Soc.* **1980**, *102*, 5798.

(11) (a) Savéant, J.-M. *J. Am. Chem. Soc.* **1987**, *109*, 6788. (b) Savéant, J.-M. *J. Am. Chem. Soc.* **1992**, *114*, 10595. (c) Andrieux, C. P.; Savéant, J.-M.; Tardy, C.; Savéant, J.-M. *J. Am. Chem. Soc.* **1998**, *120*, 4167.

(12) Similar to the formalism used for thermal outersphere electron transfers in ref 10d.

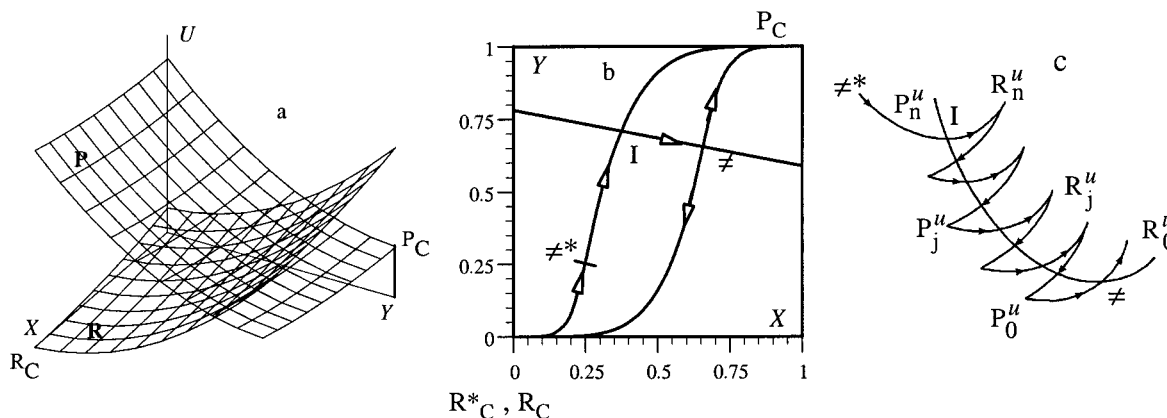


Figure 2. (a) R and P zero-order potential energy surfaces. (b) Projection of the steepest descent paths on the $X - Y$ plane. (c) Oscillatory descent from I to \neq^* .

sociative electron transfer, k_{act} is the corresponding rate constant). The two reactants may then diffuse apart from the cage, yielding D and RX with a rate constant k_{sr} , while conversely, D and RX may diffuse one toward the other, giving rise to R_C , with a rate constant k_{d} . On the product curve, P^l relaxes to the ground-state caged reactant system, P_C with a rate constant k_{-p} , while P^l may be regenerated from P_C with a rate constant k_p .

$$k_p/k_{-p} = \exp(-F\Delta G^\ddagger/RT) = k_{-act}/v_{\text{eff}}$$

(ΔG^\ddagger is the activation free energy for the recombination of the three fragments within the cage, and k_{-act} is the corresponding rate constant). The three fragments may then diffuse apart from the cage yielding D^+ , R^* , and X^- with a rate constant k_{sp} . The reverse process, where the three fragments would meet back within the same solvent cage, is negligible under usual concentration conditions. This impossibility of back-electron transfer from separated products is the key characteristic of dissociative electron transfer as opposed to stepwise reactions. Having excluded cage electron transfer between R^* and D^+ , the possibility of coupling of these two species in the solvent cage should be taken into account (rate constant: k_{cc}). Resolution of the corresponding rate equations, under the steady-state approximation, leads to eq 1 relating the quantum yield to the probability P (see Supporting Information).

$$\Phi_\infty = \frac{1}{(1+P)\left(1 + \frac{2P}{1+P} \frac{k_{-act}}{k_{\text{sp}} + k_{\text{cc}}}\right)} \quad (1)$$

In all practical cases, the ground-state electron transfer is a very uphill reaction, thus making its influence on the value of the quantum yield negligible. This simplification has been taken into account in the derivation of eq 1. The term $k_{-act}/(k_{\text{sp}} + k_{\text{cc}})$ reflects the possibility that back-electron transfer could take place within the caged fragments cluster. In a number of cases, the activation barrier for this reaction is too high for it to compete with the diffusion of the fragments out of the cage. The quantum yields then takes its maximal value, being simply given by eq 2 which reflects the funnel partitioning between products and back-electron transfer.

$$\Phi_\infty = \frac{1}{1+P} \quad (2)$$

The probability P , in eqs 1 and 2, may be related to the electronic coupling matrix element through eq 3 by application of the Landau-Zener model¹⁰ (see Supporting Information)

$$P = 1 - \exp[-\pi^{3/2}H^2/hv_{\text{eff}}(RTD)^{1/2}] \quad (3)$$

(D is the dissociation energy of the cleaving bond).

Besides bond cleavage, solvent reorganization may play an important role in the dynamics of dissociative electron transfer.^{4,11} We thus examine now whether the preceding results summarized by eqs 1–3 are still valid when the potential energy profiles (Figure 1) are replaced by potential energy surfaces involving two coordinates which represent solvent reorganization and bond stretching, respectively. We may use in this connection the same expressions of the potential energy surface that have been used previously in the modeling of thermal dissociative electron transfer,^{4,11} thus leading to the potential energy surfaces, $U_R(X,Y)$, $U_{R^*}(X,Y)$, $U_P(X,Y)$ for the three states, R ($D + RX$), R^* ($D^* + RX$), P ($D^+ + R^* + X^-$) given in eqs 4, 5, and 6, respectively.

$$U_R = \lambda_0 X^2 + DY^2 \quad (4)$$

$$U_{R^*} = U_{R^*}^0 + \lambda_0 X^2 + DY^2 \quad (5)$$

$$U_P = U_P^0 + \lambda_0(1 - X^2) + D(1 - Y^2) \quad (6)$$

where X is a fictitious charge, varying from 0 to 1, serving as index for solvent reorganization and Y is defined by eq 7.

$$Y = 1 - \exp(-\beta y) \quad (7)$$

y is the elongation of the R – X bond from its equilibrium position. $\beta = \nu_c(2\pi^2\mu/D)^{1/2}$ (ν_c : stretching frequency of the R–X bond, μ : reduced mass). λ_0 is the Marcus–Hush solvent reorganization energy,¹³ $U_{R^*}^0$ the energy of the excited state, D^* , and U_P^0 the standard energy of the ground-state reaction.

Past the transition state of the photoinduced reaction, \neq^* , the system goes down on the repulsive product surface, P, until P crosses the intersection with the reactant surface R. These two surfaces are sketched in Figure 2a. Their intersection is a parabola (the central line in Figure 2c) whose projection in the $X - Y$ plane (straight line in Figure 2b) is defined by eq 8.

$$U_P^0 = \lambda_0(2X - 1) + D(2Y - 1) \quad (8)$$

The minimum on the intersection parabola is the saddle point corresponding to the transition state of the dark reaction, noted

(13) (a) Marcus, R. A. *J. Chem. Phys.* **1956**, *24*, 4966. (b) Hush, N. S. *J. Chem. Phys.* **1958**, *28*, 962. (c) Marcus, R. A. In *Special Topics in Electrochemistry*; Rock, P. A., Ed.; Elsevier: New York, 1977; pp 161–179.

\neq in parts b and c of Figure 2. The first-order potential energy surfaces involve an upper surface associating the portions of the R and P zero-order potential energy surfaces situated above the intersection parabola and a lower surface associating the portions of the R and P zero-order potential energy surfaces situated below the intersection parabola.

The projection on the $X - Y$ plane of the steepest descent path followed by the system during the photoinduced reaction is shown in Figure 2b. Past the saddle point corresponding to the transition state of the photoinduced reaction, \neq^* , the system follows the steepest descent path on the P surface en route to the caged product state, $X = 1, Y = 1$, (eq 9) until it reaches

$$\left[\frac{1 - X}{\frac{1}{2} \left(1 + \frac{U_{R^*}^0 - U_P^0}{\lambda_0 + D} \right)} \right]_{\lambda_0}^{\frac{1}{\lambda_0}} = \left[\frac{1 - Y}{\frac{1}{2} \left(1 + \frac{U_{R^*}^0 - U_P^0}{\lambda_0 + D} \right)} \right]_{\frac{1}{D}}^{\frac{1}{D}} \quad (9)$$

the intersection between the P and R surfaces in a point noted I in Figure 2b. The fraction of the system that remains on the first-order potential energy surface, then starts an oscillatory descent from point I to the minimum \neq , as represented schematically in Figure 2c. Along this path, part of the system continuously goes to the lower first-order potential energy surface, thus partitioning between two paths, one leading to the caged product, P_C , and the other to the caged ground-state reactants, R_C . The projection on the $X - Y$ plane of the steepest descent paths from \neq to P_C and R_C (eqs 10 and 11, respectively) are shown in Figure 2b.

$$\left[\frac{1 - X}{\frac{1}{2} \left(1 + \frac{U_P^0}{\lambda_0 + D} \right)} \right]_{\lambda_0}^{\frac{1}{\lambda_0}} = \left[\frac{1 - Y}{\frac{1}{2} \left(1 + \frac{U_P^0}{\lambda_0 + D} \right)} \right]_{\frac{1}{D}}^{\frac{1}{D}} \quad (10)$$

$$\left[\frac{X}{\frac{1}{2} \left(1 + \frac{U_P^0}{\lambda_0 + D} \right)} \right]_{\lambda_0}^{\frac{1}{\lambda_0}} = \left[\frac{Y}{\frac{1}{2} \left(1 + \frac{U_P^0}{\lambda_0 + D} \right)} \right]_{\frac{1}{D}}^{\frac{1}{D}} \quad (11)$$

Along the I to \neq path, the incoming flux represented by k_0 thus partitions between a series of states, P_j^u and R_j^u of increasing stability ($j = 0$ for \neq and $j = n$ for I). The fraction, f_j , of k_0 consumed to generate P_j^u and R_j^u is proportional to $\exp(-F\Delta G_j/RT)$, where ΔG_j is the free energy corresponding to point j on the I to \neq descent ($\sum_j f_j = 1$). At each point of the I to \neq path, the system follows the set of reactions depicted in

Scheme 2 where P_j^l and R_j^l are generated and finally relax irreversibly to P_C and R_C respectively. Re-crossing of the dark reaction activation barrier from P_C and R_C and vice versa may only occur for the lowest point of the I to \neq path, that is, at the dark reaction transition state. Resolution of the ensuing set of kinetic equations (see Supporting Information) leads to the conclusion that the expression of the quantum yield (eqs 1–3) remains the same.

Conclusions

We may thus conclude that the quantum yield for photoinduced dissociative electron transfers may well be less than unity. Even in the case where associative electron transfer between the caged fragments is not able to compete with their separation, the quantum yield may reach a value as low as 0.5 according to the magnitude of the electronic coupling matrix element.¹⁴ These qualitative conclusions as well as eqs 1 and 2 relating the quantum yield to the probability that the system remains on the upper first-order curve do not hinge upon the particular model used for the potential energy surface. The accuracy of the relationship connecting this probability to the electronic coupling matrix element does depend on the model and of the approximations embodied in the semi-classical Landau–Zener theory. Application of these equations to the analysis of experimental systems will show the necessity to refine the model. The magnitude of the electronic coupling matrix element is not an easily accessible parameter. We hope that the model presented here will allow its estimation, even though approximate, and thus contribute to a better understanding of dissociative electron transfer based on the interpretation of combined photochemical and thermal (electrochemical, homogeneous) experiments.

Acknowledgment. We are indebted to Jack Kampmeier (University of Rochester) and Frank Saeva (Kodak) for the kind communication of the content of reference 2c before publication.

Supporting Information Available: Demonstration of eq 1 for both one- and two-coordinate reorganization. Demonstration of eq 3 (PDF). This material is available free of charge via the Internet at <http://pubs.acs.org>.

JA9928226

(14) For typical values of the parameters ($D = 3.5$ eV, $\nu_{\text{eff}} = 2.05 \times 10^{13}$ s⁻¹), Φ_{∞} reaches 0.51 when $H = 0.075$ eV, while $\Phi_{\infty} = 0.99$ would require H to be as low as 0.004 eV.